Journal of the Serbian Chemical Society
JSCS@tmf.bg.ac.rs • www.shd.org.rs/JSCS
J. Serb. Chem. Soc. *90* (9) 1041–1054 (2025)
JSCS–5438
Original scientific paper
Published 26 September, 2025

Dibutyltin(IV) formulations: Synthetic aspect, spectroscopic interpretation and computational calculation

SUCHITRA BUDANIA, ANKUR M KUMAR, POONAM CHAND and ASHA JAIN*

Department of Chemistry, University of Rajasthan, Jaipur-302004, Rajasthan, India

(Received 6 March, revised 15 May, accepted 10 July 2025)

Abstract: This research article reports a series of dibutyltin(IV) complexes, Bu2SnL(n)A (**1a**–**d**), synthesized by the reaction of sodium salts of substituted pyrazolones (L(n)H) and aromatic carboxylic acid (AH) with dibutyltin dichloride in dried THF solvent. The newly synthesized dibutyltin(IV) complexes were characterized by FT-IR, NMR (^{1}H, ^{13}C, ^{119}Sn) spectroscopy and mass study. The coordination mode of both ligands with central tin atom was explicated with spectroscopic analysis of the complexes. The spectroscopic results revealed that the substituted pyrazolone ligand coordinates to the tin atom in a bidentate fashion *via* enolic oxygen and a carbonyl oxygen atom. In contrast, the aromatic carboxylic acid ligand coordinates in a monodentate manner through the carboxylic oxygen atom, resulting in a penta-coordinated environment around the central tin atom. Computational calculations using density functional theory (DFT) provide insights into the optimized molecular structures, energies, Mulliken charges and distortion in bond lengths and bond angles of the newly generated complexes. The global reactivity descriptors and the frontier molecular orbitals (FMOs) were calculated to understand the structural and electronic properties of dibutyltin(IV) formulations. The theoretical study explores the proposed penta-coordinated environment around tin atoms, revealing a distortion in the geometry of the complexes.

Keywords: dibutyltin(IV) complexes; carboxylic acid; substituted pyrazolones; DFT.

INTRODUCTION

The study of organotin(IV) complexes constitutes a significant portion of organometallic chemistry and is gaining attention due to their ability to interact with various biomolecules.[1–3] Some of these complexes have demonstrated anticancer,[4–8] DNA binding,[8,9] antimicrobial,[3,7,10–12] antidiabetic,[13,14] anti-inflam-

* Corresponding author. E-mail: aashajain27@gmail.com
https://doi.org/10.2298/JSC250306051B

matory,[7,12] antituberculosis,[12,15] antileishmanial,[7] antioxidant[7,9,10,16,17] and enzyme inhibition properties.[7] The biological activity of organotin(IV) complexes is influenced by several factors such as the number of Sn–C bonds, nature of alkyl or aryl substituents attached to tin centre, coordinating ligands and the gradual hydrolytic cleavage of complexes.

Focusing on the industrial,[18] agricultural[19] and biological uses[3–17] of organotin complexes, it is crucial to comprehend their structural coordination. Advanced spectroscopic and structural approaches have been used to investigate their chemistry.[20,21] According to reported literature, many ligand systems, including Schiff bases, oximes, carboxylic acids, phenols, diketones and others, are present in structurally distinct organotin(IV) complexes.[22] The nature of ligand plays pivotal role in determining the activity of these organotin(IV) complexes as it can modify their physicochemical properties. The synergistic interaction of organotin moiety with different functional ligands has led to the development of novel complexes with enhanced pharmacological activity when compared to the corresponding free ligands.[3,11,13,15,16]

Recognizing the significance of substituted pyrazolones[23] and carboxylic acids[24] as an organic moiety, along with the substantial bioactivity of organotin complexes, our research focuses on exploring the chemistry of hybrid organotin(IV) complexes. This study involves the synthesis and structural analysis of the newly generated dibutyltin(IV) complexes using spectroscopic methods. The DFT-based quantum-chemical study gives insights into the electronic structure of molecules and their correlation with synthetic and biological properties.[3,11,13] Therefore, a conceptual computational technique, DFT integrated with experimental approach has been employed to explore global and local descriptors, as well as the structural characteristics of newly synthesized dibutyltin(IV) complexes. This combined approach provides a better understanding of electronic structure and reactivity of complexes.

EXPERIMENTAL

Mandelic acid (AH) and dibutyltin dichloride were obtained from Sigma–Aldrich Chemical Co. and utilized without additional purification. Four types of substituted pyrazolones ($L_{(1)}H$, $L_{(2)}H$, $L_{(3)}H$ and $L_{(4)}H$) were synthesized using Jensen's method.[25] The standard literature procedures were used to dry the solvents which were employed in the experimental procedure. The experimental work was carried out under a strictly anhydrous atmosphere. Tin was estimated as tin(IV) oxide. Melting points of newly synthesized complexes (**1a**–**d**) were determined in sealed capillaries. Synthesized complexes **1a**–**d** were characterized using spectroscopic techniques. IR spectra of the complexes were recorded on a Perkin Elmer – Spectrum RX-IFTIR using KBr pellets in the range 4000–400cm^{-1}. ^{1}H- and ^{13}C-NMR spectra of organotin(IV) complexes were recorded on the ECS400 MHz (JEOL) NMR spectrometer, and ^{119}Sn NMR spectrum of complex **1a** was recorded on the Bruker Advance NEO 500 MHz NMR spectrometer. Mass spectra of complexes **1a** and **1d** were carried out on Xevo G2-S Q (Tof

(Waters, USA) mass spectrometer (APCI) whereas the mass spectra of dibutyltin(IV) complexes **1b** and **1c**, were obtained using Agilant MassHunter-6470A LC/MS system using electrospray ionizaton(ESI). DFT calculation of synthesized complexes **1a**–**d** was carried out by using the DFT/B3LYP/6-31G* basis set in Spartan 20 molecular modeling software.[3,13,15,16]

The detailed synthetic procedures of dibutyltin(IV) complexes are described below.

*Synthesis of $Bu_2SnL_{(1)}A$ (**1a**)*

A dry THF solution of sterically demanding substituted pyrazolone $L_{(1)}H$ (292.2 mg, 1.35 mmol) and mandelic acid AH (205.7 mg, 1.35 mmol), was added to a methanolic solution of sodium (62.1 mg, 2.70 mmol). The reaction mixture was refluxed over a period of 6 h. Subsequently, the mixture of sodium salts of both ligands was mixed with a dry THF solution of dibutyltin dichloride (410.8 mg, 1.35 mmol). After that, the components of the reaction underwent refluxing for approximately 8 h. The solid sodium chloride (0.157 g) that was produced as a byproduct of the reaction was filtered. To get crude solid product, the volatile solvent fraction of the remaining reaction mixture was extracted at reduced pressure. A brown-colored solid product was obtained, which was recrystallized from chloroform and pet. ether mixture. Recrystallized yield = 82 %; melting point = 112 °C.

*Synthesis of $Bu_2SnL_{(2)}A$ (**1b**)*

A dry THF solution of sterically demanding substituted pyrazolone $L_{(2)}H$ (309.8 mg, 1.34 mmol) and mandelic acid AH (204.6 mg, 1.34 mmol), was added to a methanolic solution of sodium (61.8 mg, 2.68 mmol). The reaction mixture was refluxed over a period of 6 h. Subsequently, the mixture of sodium salts of both ligands was mixed with a dry THF solution of dibutyltin dichloride (408.8 mg, 1.34 mmol). After then, the components of the reaction underwent refluxing for approximately 8 h. The solid sodium chloride (0.157 g) that was produced as a byproduct of the reaction was filtered. The volatile solvent from the remaining reaction mixture was removed under reduced pressure. A brown-colored solid product was obtained, which was recrystallized from chloroform and pet. ether mixture. Recrystallized yield = 80 %; melting point = 100 °C.

*Synthesis of $Bu_2SnL_{(3)}A$ (**1c**)*

A dry THF solution of sterically demanding substituted pyrazolone $L_{(3)}H$ (368.7 mg, 1.32 mmol) and mandelic acid AH (201.5 mg, 1.32 mmol), was added to a methanolic solution of sodium (60.6 mg, 2.63 mmol). The reaction mixture was refluxed over a period of 6 h. Subsequently, the mixture of sodium salts of both ligands was mixed with a dry THF solution of dibutyltin dichloride (401.6 mg, 1.32 mmol). After then, the components of the reaction underwent refluxing for approximately 8 h. The solid sodium chloride (0.154 g) that was produced as a byproduct of the reaction was filtered. The volatile solvent from the remaining reaction mixture was removed under reduced pressure. A pale–orange-colored solid product was obtained, which was recrystallized from chloroform and pet. ether mixture. Recrystallized yield = 81 %; melting point = 108 °C.

*Synthesis of $Bu_2SnL_{(4)}A$ (**1d**)*

A dry THF solution of sterically demanding substituted pyrazolone $L_{(4)}H$ (423.0 mg, 1.35 mmol) and mandelic acid AH (205.8 mg, 1.35 mmol), was added to a methanolic solution of sodium (62.2 mg, 2.70 mmol). The reaction mixture was refluxed over a period of 6 h. Subsequently, the mixture of sodium salts of both ligands was mixed with a dry THF solution of dibutyltin dichloride (411.1 mg, 1.35 mmol). After then, the components of the reaction underwent refluxing for approximately 8 h. The solid sodium chloride (0.158 g) that was produced as a

byproduct of the reaction was filtered. The volatile solvent from the remaining reaction mixture was removed under reduced pressure. A pale–orange-colored solid product was obtained, which was recrystallized from chloroform and pet. ether mixture. Recrystallized yield = 78 %; melting point = 109 °C.

RESULTS AND DISCUSSION

Dibutyltin(IV) complexes of the type $Bu_2SnL_{(n)}A$ were synthesized by the reactions of dibutyltin dichloride with sodium salts of substituted pyrazolones ($L_{(n)}H$)) and mandelic acid (AH) in 1:1:1 mole ratio in dry refluxing THF solvent (Scheme 1).

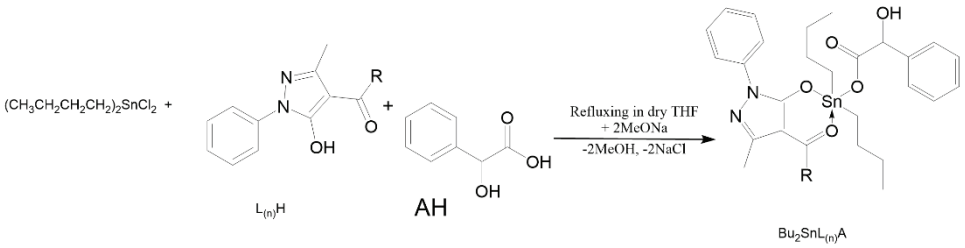

Where: R = $–CH_3$, $Bu_2SnL_{(1)}A$ (**1a**); R = $–CH_2CH_3$, $Bu_2SnL_{(2)}A$ (**1b**); R = $–C_6H_5$, $Bu_2SnL_{(3)}A$ (**1c**); R = *p*-$ClC_6H_4–$, $Bu_2SnL_{(4)}A$ (**1d**)

Scheme 1. Reactions of dibutyltin dichloride with sterically demanding substituted pyrazolones ($L_{(n)}H$) and mandelic acid (AH).

The plausible structures of synthesized dibutyltin(IV) complexes $Bu_2SnL_{(n)}A$ were elucidated by vibrational (IR), nuclear magnetic resonance (^1H, ^{13}C, ^{119}Sn) spectroscopy and mass spectrometry.

FT-IR spectra

The FT-IR spectra of the newly generated dibutyltin(IV) complexes (**1a**–**d**) have been recorded as KBr pellets in the range 4000–400 cm^{-1}. In the infrared spectra of dibutyltin(IV) complexes, the appearance of medium intensity bands in the region 655–606 cm^{-1} and 515–419 cm^{-1} may be attributed to the stretching vibrations of the Sn–O and Sn–C bonds, respectively.[26]

A band in the region of 1567–1539 cm^{-1} was seen in the IR spectra of sterically demanding substituted pyrazolones ($L_{(n)}H$), which could be attributed to carbonyl ν(>C=O) stretching vibrations.[3] This band appeared at 1531, 1529, 1533 and 1534 cm^{-1} in the IR spectra of the synthesized complexes $Bu_2SnL_{(1)}A$ (**1a**), $Bu_2SnL_{(2)}A$ (**1b**), $Bu_2SnL_{(3)}A$ (**1c**) and $Bu_2SnL_{(4)}A$ (**1d**), respectively. This shift in the position of the carbonyl ν(>C=O) stretching vibration to lower wave number indicates a bidentate nature of sterically demanding substituted pyrazolones ($L_{(n)}H$) in these complexes.

The coordination behavior of mandelic acid (AH) with tin atom is inferred from the $\nu(COO)_{asym}$ and $\nu(COO)_{sym}$ vibrations. The IR spectrum of mandelic

acid exhibited absorption bands at 1580 cm^{-1} for $\nu(COO)_{asym}$ vibration and at 1417 cm^{-1} for $\nu(COO)_{sym}$ vibration.[3] In the IR spectra of the complexes, these absorption bands appeared in the regions 1581–1564 cm^{-1} for $\nu(COO)_{asym}$ and 1384–1360 cm^{-1} for $\nu(COO)_{sym}$ vibrations. The $\Delta\nu$ ($\Delta\nu = \nu(COO)_{asym} - \nu(COO)_{sym}$) values are important data for determining the mode of bonding of carboxylates in the complexes. The calculated values of $\Delta\nu$ is of the order 193––204 cm^{-1} in the dibutyltin(IV) complexes. The increase in value of $\Delta\nu$ from 163 cm^{-1} in free mandelic acid to 193–204 cm^{-1} in dibutyltin(IV) complexes indicates the monodentate nature of carboxylic group of mandelic acid in these dibutyltin(IV) complexes.[27] A broad band appeared in the region 3478–3298 cm^{-1} in the IR spectra of the complexes, due to secondary –OH group of mandelic acid, indicates the non-involvement of this group in bonding. The absorption band appeared in the regions 1493–1415 cm^{-1} and 1601–1594 cm^{-1} may be attributed to $\nu(>C=C</>C=N–)$ and $\nu(–C_6H_5)$, respectively in the complexes.

^{1}H-NMR spectra

The ^{1}H-NMR spectrum of dibutyltin(IV) complex **1b** was recorded in $CDCl_3$ whereas, the ^{1}H-NMR spectra of dibutyltin(IV) complexes **1a**, **1c** and **1d** were recorded in $CDCl_3$ with few drops of DMSO-d_6, using TMS as an internal standard. The chemical shift values of these dibutyltin(IV) complexes are tabulated in Table S-I of the Supplementary material to this paper.

The broad signal of enolic –OH appeared in the δ region 10.67–12.77 ppm in the ^{1}H-NMR spectra of sterically demanding substituted pyrazolones ($L_{(n)}H$),[28] while the carboxylic proton (COO–H) appeared at δ 11.81 ppm in the ^{1}H-NMR spectrum of mandelic acid (AH).[3] These broad signals disappeared in the ^{1}H-NMR spectra of dibutyltin(IV) complexes which clearly show deprotonation of these ligands. The singlet observed in the ^{1}H-NMR spectra of dibutyltin(IV) complexes at δ 2.36 ppm (**1a**), 2.43 ppm (**1b**), 1.79 ppm (**1c**) and 1.82 ppm (**1d**) is due to the ring methyl protons ($–CH_3$) of substituted pyrazolone ($L_{(n)}H$) moiety. In the ^{1}H-NMR spectrum of $Bu_2SnL_{(1)}A$ (**1a**), a singlet at δ 2.39 ppm appeared for the terminal methyl protons, whereas the terminal $–CH_2CH_3$ group in the complex $Bu_2SnL_{(2)}A$ (**1b**) appeared as a quartet at δ 2.73 ppm (for CH_2 protons) and signal for CH_3 protons merged with butyl proton signals.

The signals for alcoholic –OH and –CH protons of mandelic acid were observed in the δ regions 3.64–3.73 ppm and 5.11–5.13 ppm, respectively, in the ^{1}H-NMR spectra of the complexes **1a**–**d**. Aromatic protons appeared as a multiplet in the δ region 7.17–7.89 ppm whereas protons of butyl groups, directly appended to tin, were observed in the δ region 0.66–1.68 ppm.

^{13}C-NMR spectra

The ^{13}C-NMR spectrum of dibutyltin(IV) complex **1b** was recorded in $CDCl_3$ whereas, the ^{13}C-NMR spectra of dibutyltin(IV) complexes **1a**, **1c** and **1d** were

recorded in $CDCl_3$ with few drops of DMSO-d_6, using TMS as an internal standard. Table S-II lof the Supplementary material lists the obtained chemical shift values.

In the ^{13}C NMR spectra of the sterically demanding substituted pyrazolones ($L_{(n)}H$), the signals for carbonyl (>C=O) carbon were observed at δ 196.2 ppm in $L_{(1)}H$, 197.97 ppm in $L_{(2)}H$, 192.05 ppm in $L_{(3)}H$ and 190.9 ppm in $L_{(4)}H$.[28] The positions of these carbonyl carbon (C6) signals experienced some shift in the ^{13}C-NMR spectra of dibutyltin(IV) complexes, which indicate that carbonyl group (>C=O) is participating in bonding. This suggests bidentate nature of sterically demanding substituted pyrazolone ($L_{(n)}H$). There are also some shifts observed in the positions of C_3, C_4 and C_5 carbon signals in the ^{13}C-NMR spectra of the complexes. The carboxylic carbon signal was observed at δ 173.33 in the ^{13}C-NMR spectra of mandelic acid (AH).[3] In the ^{13}C-NMR spectra of the dibutyltin(IV) complexes involving mandelic acid as a coligand, the carboxylic carbon signals are observed in the δ range 174.17–179.77 ppm. The shifting of carboxylic carbon signals indicate monodentate bonding behaviour of carboxylic group. The carbon signals of methyl group (C7) and phenyl groups are observed in the δ region 16.44––17.52 ppm and 120.92–148.97 ppm, respectively. The carbon signals of butyl groups directly bonded to tin atom appeared as splitted signals in the δ region 13.40–32.38 ppm in ^{13}C-NMR spectra of the dibutyl(IV) complexes (Table S-II).

^{119}Sn-NMR spectrum

The ^{119}Sn-NMR chemical shift (^{119}Sn) values provide insights into the geometry and the coordination number of tin in organotin(IV) complexes. The ^{119}Sn--NMR spectrum of dibutyltin(IV) complex **1a** was recorded in DMSO-d_6. The ^{119}Sn chemical shift value of dibutyltin(IV) complex $Bu_2SnL_{(1)}A$ (**1a**) is observed at δ – 125.86 ppm. This ^{119}Sn-NMR value reveals the presence of five coordinated tin centre in dibutyltin(IV) complex.[29] The coordination sphere of tin consists of two butyl groups, a chelating *O*,*O*'-bidentate substituted pyrazolone ($L_{(n)}H$) and a monodentate mandelic acid (AH).

Mass spectra

The mass spectral data of dibutyltin(IV) complexes **1a** and **1d**, were obtained using Xevo G2-S Q (Tof, Waters, USA) mass spectrometer (APCI), whereas the mass spectral data of dibutyltin(IV) complexes **1b** and **1c**, were obtained using Agilant MassHunter-6470A LC/MS system using electrospray ionization (ESI). The obtained ion peaks (*m*/*z* values) along with their intensity in % are presented in the Table S-III of the Supplementary material.

The mass spectrum of dibutyltin(IV) complex **1a** exhibits low-intensity molecular ion peak, $[M]^+$. The mass spectral data for complexes **1a**–**d** reveal a similar

fragmentation pattern. The resulting fragments closely match the anticipated structures of complexes. The absence of high intensity peaks in the *m*/*z* region above the molecular weight of complexes, indicates the monomeric nature of the dibutyltin(IV) complexes.

The obtained results of vibrational (IR), nuclear magnetic resonance (^{1}H, ^{13}C, ^{119}Sn) spectroscopies and mass spectrometry suggested a penta-coordinated geometry for tin in these complexes (Fig. 1).

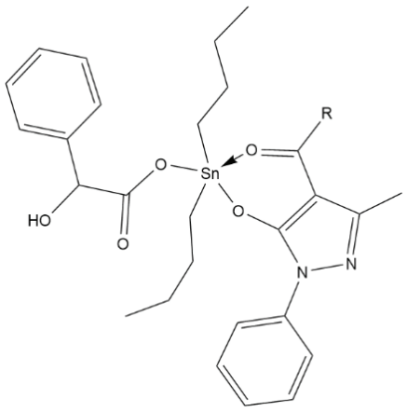

Fig. 1. Structure of dibutyltin(IV) complexes of sterically demanding substituted pyrazolone and mandelic acid, where: R = -CH_3, $Bu_2SnL_{(1)}A$ (**1a**); R = –CH_2CH_3 , $Bu_2SnL_{(2)}A$ (**1b**); R = –C_6H_5, $Bu_2SnL_{(3)}A$ (**1c**); R = *p*-ClC_6H_4–, $Bu_2SnL_{(4)}A$ (**1d**).

DFT calculations

The optimized molecular structures and molecular properties of synthesized dibutyltin(IV) complexes, $Bu_2SnL_{(n)}A$ (**1a**–**d**) have been studied in gas phase, using DFT-B3LYP functional in Spartan 20 computational modeling software. The ground state energy, E_{HOMO}, E_{LUMO}, dipole moment and other global reactivity parameters of the complexes $Bu_2SnL_{(n)}A$ have been calculated and obtained data are summarized in Table I.

Fig. 2 represents the optimized structures of the dibutyltin (IV) complexes $Bu_2SnL_{(n)}A$ (**1a**–**d**). The ground state energy of the synthesized complex $Bu_2SnL_{(4)}A$ (**1d**) is –2229.09439 a.u., the lowest among all the complexes, indicating that $Bu_2SnL_{(4)}A$ (**1d**) is the most stable complex. The ability to donate electron is associated with E_{HOMO}, while the ability to accept electrons is linked to the E_{LUMO}.[30] Furthermore, the energy gap between HOMO and LUMO serve as key indicator of the reactivity of the complexes.

The ΔE gap is found to be 3.88 eV for the complex $Bu_2SnL_{(4)}A$ (**1d**) which is lowest among all the complexes. The lowest ΔE gap suggests the highest reactivity of this complex. As shown in Figs. 3 and 4, the charge density of HOMO in complexes **1a**–**c** is localized on the five membered pyrazole ring having phenyl group forming a delocalized π system, whereas in complex **1d**, the charge density of

HOMO is mainly localized on the five membered pyrazole ring having phenyl group and phenyl ring of mandelic acid moiety.

TABLE I. Selected molecular properties of optimized geometries of dibutyltin(IV) complexes; $IP = -E_{HOMO}$; $EA = -E_{LUMO}$; $\mu = -(IP + EA)/2$; $\chi = (IP + EA)/2$; $\eta = (IP - EA)/2$; $S = 1/2\eta$[30]

Property	Complex **1a** $Bu_2SnL_{(1)}A$	Complex **1b** $Bu_2SnL_{(2)}A$	Complex **1c** $Bu_2SnL_{(3)}A$	Complex **1d** $Bu_2SnL_{(4)}A$
Molecular formula	$C_{28}H_{36}N_2O_5Sn$	$C_{29}H_{38}N_2O_5Sn$	$C_{33}H_{38}N_2O_5Sn$	$C_{33}H_{37}ClN_2O_5Sn$
Molecular weight	599.300	613.327	661.371	695.816
Energy, a.u.	–1577.76033	–1617.07528	–1769.49513	–2229.09439
E_{HOMO} / eV	–6.05	–5.91	–6.03	–6.11
E_{LUMO} / eV	–1.53	–1.58	–1.88	–2.23
ΔE / eV	4.52	4.33	4.15	3.88
Dipole moment, D	2.77	3.92	1.96	5.26
Polarizability	84.70	86.23	90.14	91.38
Ionization potential, eV	6.05	5.91	6.03	6.11
Electron affinity, eV	1.53	1.58	1.88	2.23
Chemical potential, μ	–3.79	–3.745	–3.955	–4.17
Elecrtonegativity, χ	3.79	3.745	3.955	4.17
Chemical hardness, η	2.26	2.165	2.075	1.94
Chemical softness, S	0.2212	0.2309	0.2409	0.2577
Area, Å^2	577.93	601.34	638.82	656.87
Volume, Å^3	547.22	565.63	613.19	627.71
PSA / Å^2	59.977	59.619	59.138	59.371
Ovality	1.79	1.82	1.83	1.85

For the LUMO of complexes **1a**–**d**, the charge density is localized on five membered pyrazole ring and carbonyl carbon of substituted pyrazolone moiety. This theoretical study reveals that localization of charge density on substituted pyrazolone moiety plays a crucial role for determining the reactivity of dibutyltin(IV) complexes.

The optimized molecular structure of the complexes $Bu_2SnL_{(n)}A$ (**1a**–**d**) have been studied, and the selected bond lengths and bond angles are listed in Tables II and III, respectively.

In the optimized structures of dibutyltin complexes (**1a**–**d**), the sum of the equatorial angles 108.98 (C9–Sn1–C13), 87.62 (C9–Sn1–O2) and 163.35° (C13––Sn1–O2) is 359.95° in complex **1a,** 110.95 (C10–Sn1–C14), 89.68 (C14–Sn1––O1) and 158.96° (C10–Sn1–O1) is 359.59° in complex **1b**, 113.90 (C5–Sn1––C12), 92.18 (C12–Sn1–O3) and 153.61° (C5–Sn1–O3) is 359.69° in complex **1c**, and 132.61 (C7–Sn1–C11), 109.68 (C7–Sn1–O3) and 115.95° (C11–Sn1–O3) is 358.24° in complex **1d**. The O–Sn–O bond angle between axial positions are 148.04° (O1–Sn1–O3) in complex **1a**, 149.42° (O2–Sn1–O3) in complex **1b**, 152.00° (O2–Sn1–O1) in complex **1c** and 167.53° (O4–Sn1–O2) in complex **1d**.

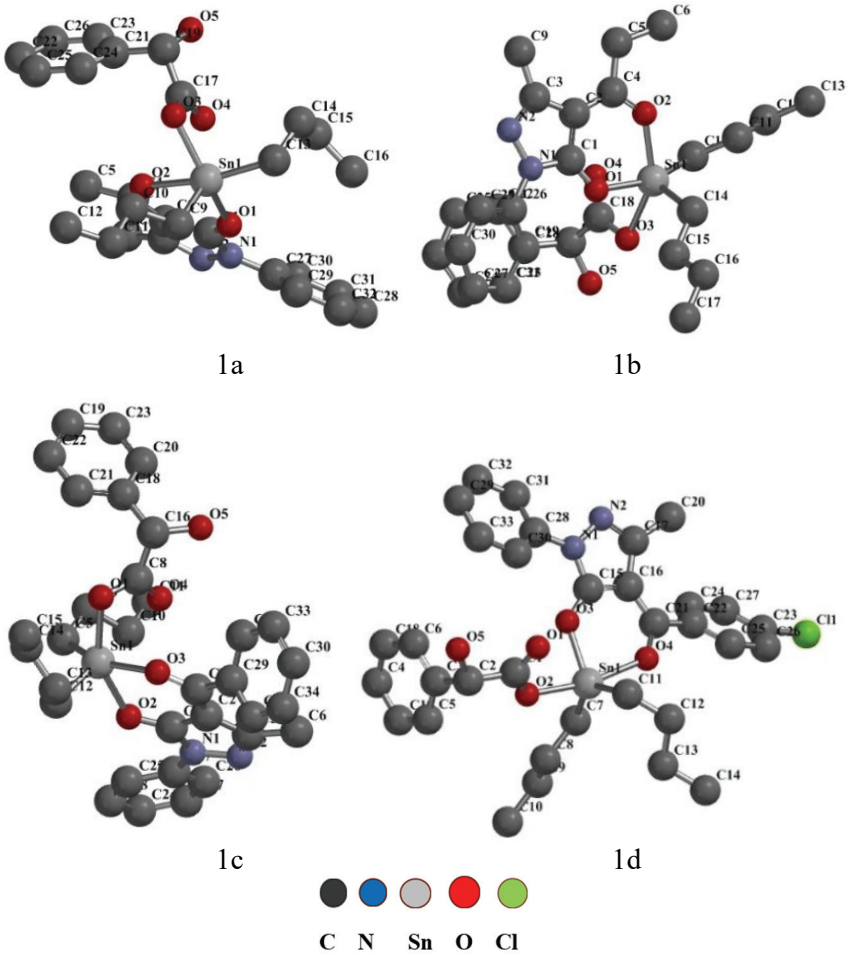

Fig. 2. The optimized molecular structures of dibutyltin(IV) complexes $Bu_2SnL_{(n)}A$ (**1a**–**d**).

These observations suggest that carbon atoms of two butyl groups and covalently bonded oxygen atom of substituted pyrazolone occupy the equatorial plane with tin atom, whereas the axial position were occupied by second oxygen atom of substituted pyrazolone and oxygen atom of carboxylate group. Thus, a distorted trigonal bipyramidal geometry may be suggested for these dibutyltin(IV) complexes (Fig. 2).

The theoretically calculated Mulliken charge at selected atoms in dibutyltin(IV) formulations have been depicted in Table IV. The charge distribution analysis reveals that the positively charged tin atom is surrounded by negatively charged carbon (from butyl groups) and oxygen (from substituted pyrazolones and carboxylic acid) atoms.

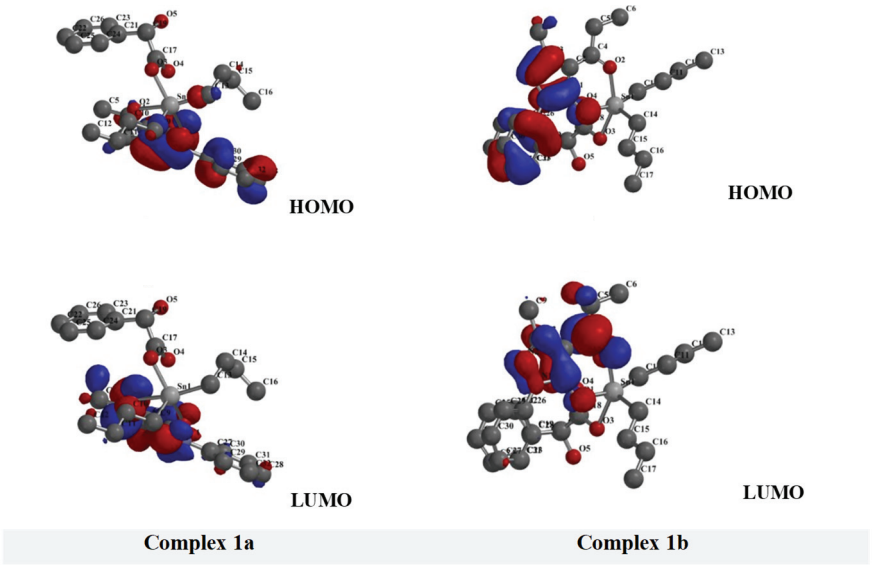

Fig. 3. FMOs of optimized molecular geometries of dibutyltin(IV) complexes (**1a**,**1b**)

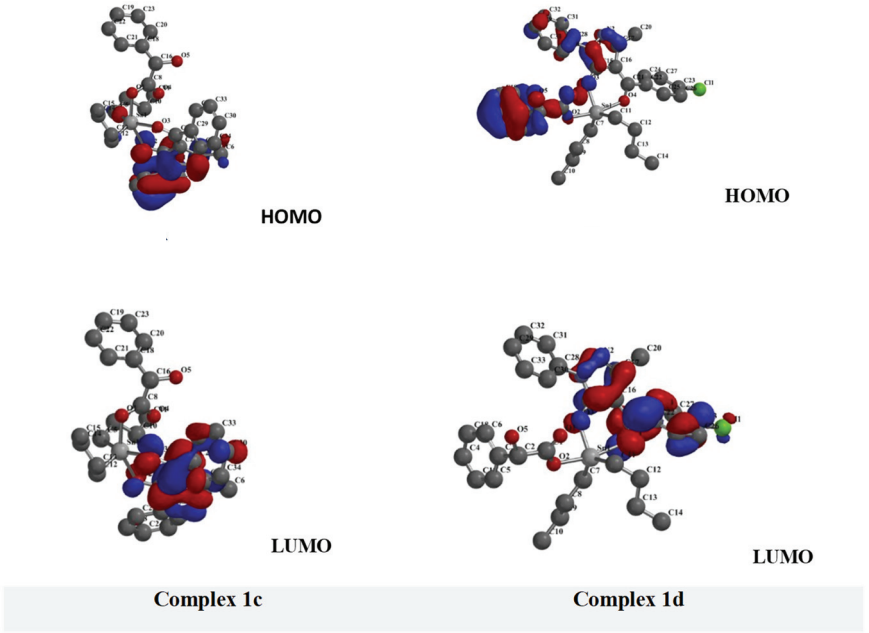

Fig. 4. FMOs of optimized molecular geometries of dibutyltin(IV) complexes (**1c** and **d**).

The negative charge on oxygen atoms of substituted pyrazolone (–0.736(O1), –0.637(O2) in complex **1a**, –0.720(O2), –0.661(O1) in complex **1b**, –0.724(O2),

-0.660(O3) in complex **1c** and –0.737(O3), –0.638(O4) in complex **1d**) is higher compared to oxygen atom of carboxylic acid (–0.627(O3) in complex **1a**, -0.654(O4) in complex **1b**, –0.653(O1) in complex **1c** and –0.687(O2) in complex **1d**) indicate stronger bonding interaction between substituted pyrazolone and tin atom.

TABLE II. Selected bond distances (in Å) of optimized geometries of dibutyltin(IV) complexes (**1a -1d**)

Complex **1a** $Bu_2SnL_{(1)}A$	Complex **1b** $Bu_2SnL_{(2)}A$	Complex **1c** $Bu_2SnL_{(3)}A$	Complex 1**d** $Bu_2SnL_{(4)}A$
2.153 (Sn1–C9)	2.152 (Sn1–C14)	2.150 (Sn1–C12)	2.136 (Sn1–C7)
2.162 (Sn1–C13)	2.158 (Sn1–C10)	2.157 (Sn1–C5)	2.143 (Sn1–C11)
2.104 (Sn1–O1)	2.135 (Sn1–O1)	2.139 (Sn1–O2)	2.042 (Sn1–O3)
2.192 (Sn1–O2)	2.153 (Sn1–O2)	2.140 (Sn1–O3)	2.265 (Sn1–O4)
2.188 (Sn1–O3)	2.195 (Sn1–O3)	2.133 (Sn1–O1)	2.074 (Sn1–O2)
1.276(O3–C17)	1.285(O3–C18)	1.288(O1–C8)	1.301(O2–C1)
1.263(C17=O4)	1.258(C18=O4)	1.248(C8=O4)	1.234(C1=O1)
1.291 (O1–C1)	1.281 (O1–C1)	1.285 (O2–C1)	1.296 (O3–C15)
1.429 (C1=C2)	1.432 (C1=C2)	1.432(C1=C2)	1.429 (C15=C16)
1.412 (C2–C4)	1.406(C2–C4)	1.405 (C2–C7)	1.416 (C16–C21)
1.272 (C4=O2)	1.281 (C4=O2)	1.281 (C7=O3)	1.273 (C21=O4)

TABLE III. Selected bond angles (in °) of optimized geometries of dibutyltin(IV) complexes (**1a**–**d**)

Complex **1a** $Bu_2SnL_{(1)}A$	Complex **1b** $Bu_2SnL_{(2)}A$	Complex **1c** $Bu_2SnL_{(3)}A$	Complex **1d** $Bu_2SnL_{(4)}A$
108.98(C9–Sn1–C13)	110.95(C10–Sn1–C14)	113.90(C5–Sn1–C12)	132.61(C7–Sn1–C11)
87.62(C9–Sn1–O2)	89.68(C14–Sn1–O1)	92.18(C12–Sn1–O3)	109.68(C7–Sn1–O3)
163.35(C13–Sn1–O2)	158.96(C10–Sn1–O1)	153.61(C5–Sn1–O3)	115.95(C11–Sn1–O3)
94.48(C13–Sn1–O1)	87.77(C10–Sn1–O2)	90.36(C5–Sn1–O2)	85.98(C7–Sn1–O4)
96.29(C13–Sn1–O3)	97.60(C10–Sn1–O3)	96.68(C5–Sn1–O1)	94.42(C7–Sn1–O2)
82.29(O2–Sn1–O1)	82.28(O1–Sn1–O2)	81.51(O2–Sn1–O3)	86.14(O2–Sn1–O3)
148.04(O1–Sn1–O3)	149.42(O2–Sn1–O3)	152.00(O2–Sn1–O1)	167.53(O4–Sn1–O2)
78.83(O3–Sn1–O2)	82.26(O3–Sn1–O1)	80.23(O1–Sn1–O3)	82.01(O3–Sn1–O4)
119.94(O3–C17=O4)	119.51(O3–C18=O4)	121.84(O1–C8=O4)	125.05(O2–C1=O1)
126.52(Sn1–O1–C1)	126.41(Sn1–O1–C1)	125.61(Sn1–O2–C1)	129.51(Sn1–O3–C15)
130.62(O1–C1=C2)	130.01(O1–C1=C2)	129.58(O2–C1=C2)	131.00(O3–C15=C16)
122.60(C1=C2–C4)	122.67(C1=C2–C4)	121.94(C1=C2–C7)	121.76(C15=C16–C21)
121.78(C2–C4=O2)	122.19(C2–C4=O2)	122.31(C2–C4=O3)	121.55(C16–C21=O4)
132.42(C4=O2–Sn1)	133.28(C4=O2–Sn1)	133.26(C7=O3–Sn1)	131.96(C21=O4–Sn1)

This observation is further supported by mass spectral data. The presence of a peak at *m*/*z* 449.2868 (100 % intensity) in complex **1a**, 463.6000 (16.66 % intensity) in complex **1b**, 511.9000 (6.66 % intensity) in complex **1c** and 545.6388 (72.72 % intensity) in complex **1d** corresponds to $[M\text{-}A]^+$ fragment ion (Table S-

-III). This indicates strong bonding interaction between oxygen atom of substituted pyrazolone and tin atom.

TABLE IV. Mulliken atomic charge on selected atoms of dibutyltin(IV) formulations(**1a-1d**)

Complex **1a** $Bu_2SnL_{(1)}A$	Complex **1b** $Bu_2SnL_{(2)}A$	Complex **1c** $Bu_2SnL_{(3)}A$	Complex **1d** $Bu_2SnL_{(4)}A$
+1.574 (Sn1)	+1.562(Sn1)	+1.557 (Sn1)	+1.539 (Sn1)
–0.650 (C9)	–0.649 (C26)	–0.655 (C12)	–0.654 (C7)
–0.647 (C13)	–0.637 (C22)	–0.640 (C5)	–0.643 (C11)
–0.736(O1)	–0.720(O2)	–0.724(O2)	–0.737(O3)
+0.683(C1)	+0.690(C13)	+0.692(C1)	+0.679(C15)
–0.117(C2)	–0.115(C12)	–0.111(C2)	–0.124(C16)
+0.436(C4)	+0.437(C11)	+0.337(C3)	+0.333(C21)
–0.637(O2)	–0.661(O1)	–0.660(O3)	–0.638(O4)
–0.627(O3)	–0.654(O4)	–0.653(O1)	–0.687(O2)
+0.665(C17)	+0.661(C21)	+0.661(C8)	+0.641(C1)
–0.608(O4)	–0.579(O5)	–0.673(O4)	–0.533(O1)

CONCLUSION

Four dibutyltin(IV) complexes (**1a**–**d**) were synthesized, and their structures elucidated using spectroscopic evidences and DFT-B3LYP functional. The synthetic method included incorporation of dibutyltin(IV) into structurally different substituted pyrazolone and mandelic acid, resulting in the formation of hybrid dibutyltin(IV) formulations. ^{119}Sn-NMR chemical shift value revealed the presence of pentacoordinated tin centre in the dibutyltin(IV) complex. DFT/B3LYP functional was used for the theoretical investigation of dibutyltin(IV) complexes, $Bu_2SnL_{(n)}A$. Optimized molecular structure, optimized energy and other global reactivity parameters of the complexes were studied. The Mulliken charge distribution analysis of dibutyltin(IV) complexes reveals the charge distribution on various atoms of complexes. On the basis of spectroscopic and theoretical evidences**,** a distorted trigonal–bipyramidal geometry was proposed in which substituted pyrazolone acts as bidentate ligand, coordinating through enolic oxygen (–O) as well as carbonyl (>C=O) oxygen, while the mandelic acid acts as monodentate ligand coordinating through carboxylic –C(O)O group.

SUPPLEMENTARY MATERIAL

Additional data and information are available electronically at the pages of journal website: https://www.shd-pub.org.rs/index.php/JSCS/article/view/13280, or from the corresponding author on request.

Acknowledgements. All authors are thankful to the Head, Department of Chemistry, University of Rajasthan, Jaipur, India, for providing necessary research facilities and MRC, MNIT, Jaipur and SAIF, Panjab University, Chandigarh, for providing facilities for spectroscopic analysis.

ИЗВОД

ДИБУТИЛКАЛАЈ(IV) ФОРМУЛАЦИЈЕ: СИНТЕТИЧКИ АСПЕКТ, СПЕКТРОСКОПСКА ИНТЕРПРЕТАЦИЈА И КОМПЈУТЕРСКА КАЛКУЛАЦИЈА

SUCHITRA BUDANIA, ANKUR M KUMAR, POONAM CHAND и ASHA JAIN

Department of Chemistry, University of Rajasthan, Jaipur-302004, Rajasthan, India

Овај истраживачки чланак приказује серију дибутилкалај(IV) комплекса, $Bu_2SnL_{(n)}A$ (**1a**–**d**), синтетисаних реакцијом натријумових соли супституисаних пиразолона ($L_{(n)}H$) и ароматичне карбоксилне киселине (AH) са дибутилкалај-дихлоридом у сувом THF растварачу. Новосинтетисани дибутилкалај(IV) комплекси су окарактерисани FT-IR, NMR (^1H, ^{13}C, ^{119}Sn) спектроскопијом и масеном анализом. Мод координације оба лиганда са централним атомом калаја објашњен је спектроскопском анализом комплекса. Спектроскопски резултати су открили да се супституисани пиразолонски лиганд координише са атомом калаја на бидентатни начин преко енолног кисеоника и карбонилног атома кисеоника. Насупрот томе, лиганд ароматичне карбоксилне киселине координише се монодентатно преко карбоксилног атома кисеоника, што резултира пентакоординационим окружењем око централног атома калаја. Рачунске калкулације коришћењем теорије функционала густине (DFT) пружају увид у оптимизоване молекуларне структуре, енергије, Маликенова наелектрисања и дисторзије у дужинама и угловима веза новоформираних комплекса. Дескриптори глобалне реактивности и граничне молекуларне орбитале (FMO) су израчунати како би се разумеле структурне и електронске особине дибутилкалај(IV) формулација. Теоретска студија истражује предложено пентакоординационо окружење око атома калаја, откривајући дисторзију у геометрији комплекса.

(Примљено 6. марта, ревидирано 15. маја, прихваћено 10. јула 2025)

REFERENCES

1. K. Ullah, S. Ali, A. Haider, S. Naz, S. Yousuf, K.S. Munawar, M. S. Jan, R. Zafar, R. Kumar, *J. Mol. Struct.* **1322** *(*2025**)** 140444 (https://doi.org/10.1016/j.molstruc.2024.140444)
2. M. S. Mansour, A. T. Ibrahium, A.A. El-Sherif, W. H. Mahmoud, *Appl. Organomet. Chem.* **38** (2024) e7656 (https://doi.org/10.1002/aoc.7656)
3. S. Budania, S. Saxena, A. Jain, *J. Indian Chem. Soc.* **101** (2024) 101198 (https://doi.org/10.1016/j.jics.2024.101198)
4. J. Devi, A. Boora, M. Rani, T. Arora, *Anti-Cancer Agents Med. Chem* **23** (2023) 164 (https://doi.org/10.2174/1871520622666220520095549)
5. X. M. Du, J. W. Ma, Q. L. Li, Y. Cui, C. L. Ma, *Appl. Organomet. Chem.* **38** (2024) e7522 (https://doi.org/10.1002/aoc.7522)
6. D. A. Berseneva, D. B. Shpakovsky, E. A. Nikitin, V. E. Goncharenko, Y. A. Gracheva, K. A. Lyssenko, Y. F. Oprunenko, E. R. Milaeva, *Russ. J. Coord. Chem.* **49** (2023) 622 (https://doi.org/10.1134/S1070328423600559)
7. S. Rahim, A. Sadiq, A. Javed, M. Kubicki, B. Kariuki, M. Assad, N. Muhammad, N. Fatima, M. Khan, A. F. AlAsmari, F. Alasmari, *J. Mol. Struct.* **1313** (2024) 138703 (https://doi.org/10.1016/j.molstruc.2024.138703)
8. M. Pooyan, Z. Shariatinia, F. Mohammadpanah, K. Gholivand, M. Dusek, V. Eigner, M. Satari, A. A. E. Valmoozi, *J. Mol. Liq.* **391** (2023) 123442 (https://doi.org/10.1016/j.molliq.2023.123442)

9. S. Ramzan, S. Rahim, S. T. Hussain, K. B. Holt, J. K. Cockcroft, N. Muhammad, Z. Ur--Rehman, A. Nawaz, S. Shujah, *Appl. Organomet. Chem.* **37** (2023) e7161 (https://doi.org/10.1002/aoc.7161)
10. S. Saroya, S. Asija, N. Kumar, Y. Deswal, *J. Indian Chem. Soc.* **99** (2022) 100379 (https://doi.org/10.1016/j.jics.2022.100379)
11. A. Sharma, A. Jain, S. Saxena, *Appl. Organomet. Chem.* **29** (2015) 499 (https://doi.org/10.1002/aoc.3321)
12. A. Boora, J. Devi, B. Kumar, B. Taxak, *BioMetals* **38** (2025) 153 (https://doi.org/10.1007/s10534-024-00644-8)
13. A. Kumawat, K. Soni, S. Saxena, A. Jain, *Appl. Organomet. Chem., C* **37** (2023) e7205 (https://doi.org/10.1002/aoc.7205)
14. P. Debnath, K. S. Singh, T. S. Devi, S. S. Singh, R. J. Butcher, L. Sieroń, W. Maniukiewicz, *Inorg. Chim. Acta* **510** (2020) 119736 (https://doi.org/10.1016/j.ica.2020.119736)
15. K. Soni, A. Kumawat, S. Saxena, A. Jain, *Bull. Chem. Soc. Jpn.* **97** (2024) 9 (https://doi.org/10.1093/bulcsj/uoae056)
16. A. M. Kumar, S. Budania, A. Jain, *Synth. Commun.* **54** (2024) 390 (https://doi.org/10.1080/00397911.2024.2306641)
17. S. Saroya, S. Asija, N. Kumar, Y. Deswal, *J. Indian Chem. Soc.* **99** (2022) 100379 (https://doi.org/10.1016/j.jics.2022.100379)
18. W. T. Piver, *Environ. Health Persp.* **4** (1973) 61 (https://ehp.niehs.nih.gov/doi/pdf/10.1289/ehp.730461)
19. M. Hoch, *Appl. Geochem.* **16** (2001) 719 (https://doi.org/10.1016/S0883-2927(00)00067-6)
20. S. Iftikhar, S. Hussain, S. Murtaza, D. Ali, S. Yousuf, M. A. Ali, A. Haider, M. Shahid, A. M. Alsuhaibani, M. S. Refat, *Appl. Organomet. Chem.* **38** (2024) e7581 (https://doi.org/10.1002/aoc.7581)
21. Y. Tan, Z. Zhang, J. Liu, Y. Tan, W. Jiang, *J. Mol. Struct.* **1322** (2025) 140697 (https://doi.org/10.1016/j.molstruc.2024.140697)
22. L. Pellerito, L. Nagy, *Coord. Chem. Rev.* **224** (2002) 111 (https://doi.org/10.1016/S0010-8545(01)00399-X)
23. F. Marchetti, C. Pettinari, C. Di Nicola, A. Tombesi, R. Pettinari, *Coord. Chem. Rev.* **401** (2019) 213069 (https://doi.org/10.1016/j.ccr.2019.213069)
24. M. Sirajuddin, S. Ali, A. Shahnawaz, F. Perveen, S. Andleeb, S. Ali, *J. Mol. Struct.* **1207** (2020) 127809 (https://doi.org/10.1016/j.molstruc.2020.127809)
25. B. S. Jensen, *Acta Chem. Scand*. **13** (1959) 1668 (https://doi.org/10.3891/acta.chem.scand.13-1668)
26. S. Sharma, A. Jain, S. Saxena, *Main Group Met. Chem.* **30** (2007) 63 (https://doi.org/10.1515/MGMC.2007.30.2-3.63)
27. G. B. Deacon, R. J. Phillips, *Coord. Chem. Rev.* **33** (1980) 227 (https://doi.org/10.1016/S0010-8545(00)80455-5)
28. R. K. Gupta, A. Jain, S. Saxena, *Main Group Met. Chem.* **33** (2010) 167 (https://doi.org/10.1515/mgmc.2010.33.4-5.167)
29. A. Joshi, S. Verma, A. Jain, S. Saxena, *Main Group Met. Chem.* **28** (2005) 31 (https://doi.org/10.1515/MGMC.2005.28.1.31)
30. S. Budania, S. Saxena, A. Jain, *IOP Conf. Ser. Mater. Sci. Eng.* **1248** (2022) 012106 (https://doi.org/10.1088/1757-899X/1248/1/012106).